ELSEVIER

Journal of Electroanalytical Chemistry 390 (1995) 135–142

JOURNAL OF ELECTROANALYTICAL CHEMISTRY

Absorption–desorption of deuterium at Pd95%–Rh5% alloy I: environment and temperature effects

G. Mengoli [a], M. Fabrizio [a], C. Manduchi [b], E. Milli [b], G. Zannoni [b]

[a] *IPELP CNR, C. so Stati Uniti 4, 35020 Padua, Italy*
[b] *Dipartimento di Fisica "G. Galilei", via Marzolo 8, 35131 Padua, Italy*

Received 15 April 1994; in revised form 30 January 1995

Abstract

The gas phase and electrolytic loading of Pd95%–Rh5% alloy with deuterium were investigated. Gas loading was carried out isochorically under 900 mbar D_2, by decreasing the temperature from 900 °C to 20 °C. Although some D_2 was absorbed from high temperatures downwards, most of the absorption was measured at 20 °C, at which the [D]/[Me] (deuterium to metal atom) ratio exceeded the value typical for pure Pd. When the alloy deuterides were heated from 20 °C to 900 °C, they where found to decompose for temperatures below 100 °C, but some deuterium was still absorbed at high temperatures. The electrolytic insertion of deuterium was carried out potentiostatically in alkaline D_2O electrolytes, the amount of deuterium loaded being determined by anodic extraction afterwards. The maximum [D]/[Me] ratios thus achieved at 25 °C, which exceeded those obtained by gas loading, were found to increase with the alkalinity of the electrolyte. With electrolytic insertion at 90 °C, alloy deuterides of large [D]/[Me] ratio could be obtained which, in the electrolytic environment, showed a thermal decomposition rate much slower than that tested in gas phase desorption experiments.

Keywords: Deuterium absorption; Desorption; Pd–Rh alloy

1. Introduction

The solubility of hydrogen in Pd and the stability of Pd hydrides are affected by the presence of a third substitutional element in the Pd lattice: the type and extent of the effects depend, sometimes in an unexpected way, on the nature and concentration of the substitutional element.

As regards alloys of Pd with noble metals, those with Ag and Au behave similarly towards hydrogen: both substitutional elements compete with hydrogen by adding s electrons to the collective sd band of Pd and correspondingly decrease the overall solubility of hydrogen [1–6]. Instead, since the parameters of the host lattice are enlarged by alloyed Ag or Au, hydrogen accommodates in the interstitial sites better than in Pd, as indicated by the increased exothermicity of hydrogen absorption [1–6].

Significant differences in the interaction with hydrogen are observed for Pd alloys with either Pt or Rh substituted, although these metals are of the same group as Pd. Not only do Pd–Pt alloys absorb less hydrogen than pure Pd, but the solubility of hydrogen decreases much more than linearly with Pt content, as the corresponding hydrides have higher and higher decomposition pressures [1,7]. Instead, at room temperature, Pd–Rh alloys dissolve more hydrogen than pure Pd, notwithstanding the low exothermicity of hydride formation, and decomposition pressures which are higher than those of Pd hydrides.

All investigations carried out using various hydrogen insertion techniques [7–11] confirm these peculiarities of Pd–Rh alloys, whereas there is some disagreement about the extent of the effects observed for various Rh contents in alloys. Thus (by electrochemical insertion) Green and Lewis [9] exceeded the [H]/[Me](hydrogen to metal) atomic ratio typical of pure Pd with alloys with relatively low Rh contents (maximum absorption at 2.7% Rh). Conversely, Baranowski et al. [11] achieved [H]/[Me] = 0.9 to 1.0 with alloys containing $5\% \leq [Rh] \leq 40\%$ loaded under H_2 pressures in the range 2×10^4 to 2×10^3 atm, the alloys with higher Rh contents becoming fully loaded at lower pressures. The reasonable conclusion of the latter

SSDI 0022-0728(95)03945-7

finding was that Rh, although it does not form hydrides in its pure state, behaves as a hydrogen absorber when placed in the Pd lattice.

All the above results refer to light hydrogen; to our knowledge, no systematic investigation on deuterium absorption at Pd–Rh alloys has yet been performed. Substituting deuterium for hydrogen is not trivial, because the two isotopes behave differently with Pd: mobility within the Pd lattice and decomposition pressures are different, and in general Pd dissolves less deuterium than hydrogen.

The present paper deals with the insertion of deuterium (performed by loading from the gas phase as well as electrochemically) into Pd95%–Rh5% alloy, which was chosen as a compromise between the percentages used in the experiments of Lewis and Baranowski.

2. Experimental

2.1. Materials

The Pd95%–Rh5% alloy (Franco Suisse) was cast from 99.9% purity metals (Pd from a Russian company and Rh from Metalli Preziosi); the cast alloy was then cold worked and shaped into sheets of various thicknesses which were then annealed at 900 °C under Ar atmosphere. D_2O (Aldrich) was 99.9% isotopic purity; H_2O was Millipore grade; electrolytes Li_2O (Alpha) and Li_2SO_4 (Merck) were reagent grade; D_2 (Alphagaz) was 99.9% isotopic purity.

2.2. Apparatus and procedures

2.2.1. Loading by D_2

The reaction chamber consisted of a quartz tube sealed at the bottom ($\phi = 4$ cm, $h = 30$ cm). The lower part of the tube ($h = 12$ cm) was dipped in a thermostated oven and could be maintained at temperatures in the range 20–900 °C. The temperature of the tube was taken from oven to room temperature both by the insulating wall of the oven ($h = 3$ cm) and a mantle of cooling water ($h = 12$ cm) flowing inside a stainless steel jacket round the tube. The upper part of the tube ($h = 3$ cm) was fitted to the vacuum line (or gas supply line) by a series of high-vacuum sealing o-rings. The core of the vacuum or gas supply system was a chamber constituting either pre-high vacuum buffer (operated by two rotative pumps) or gas reservoir. Both the latter and the reaction chamber could be interconnected selectively to several lines, for example a diffusion pump, which could achieve a vacuum of less than or equal to 10^{-6} mbar, vacuum meters (Pirani and cold device), gas inlet, and a high-precision mechanical manometer, the barometric fluctuations of which were corrected by the second manometer in air.

Loading–unloading experimental procedures were as follows:

alloy samples (sheets) were placed in the reaction chamber and vacuum annealed at 900 °C for several hours, the temperature near the sample (at a distance 0.2 to 0.3 cm) was measured with a W–Re thermocouple;

sample surfaces were reduced by a D_2 draft at 900 °C for 2 h, followed by gas evacuation;

900 mbar D_2 were then allowed to enter the system and absorption was determined isochorically from the pressure drop when the temperature decreased slowly (about 30 h) from 900 to 20 °C;

D_2 desorption was measured similarly, simply by reversing the thermal process from 20 °C to 900 °C at a heating rate of less than or equal to 0.5 °C min^{-1}.

The above measurements were preceded by standardization of the system without sample to determine, as the temperature of the oven decreased from 900 to 20 °C, the pressure drop due to D_2 cooling. This (confirmed by reversing the thermal cycle to 900 °C) was used to correct the absorption measured with the alloys.

2.2.2. Electrochemical loading

Flag alloy sheet electrodes approximately 1.0×1.0 cm^2, 0.02 cm thick, made as described elsewhere [12] were used for electrochemical loading–unloading experiments. Each electrode was assembled in a double-jacketed 50 ml capacity cell in which a Pt coil wrapped round the flag acted as the counter electrode; the reference electrode was an SCE in which the original solution had been replaced by KCl-saturated D_2O. A reference composed of an Ag coil (0.1 V positive vs. SCE) was also used in experiments above room temperature. The cell was thermostated at either 25 °C or 90 °C by an Haake F3 thermostat. To avoid loss by evaporation, the gas exit of the cell was equipped with a refrigerator, allowing condensed D_2O to reflow into the cell. The electrolytic apparatus from Amel consisted of a model 731 integrator and a model 566 wave-form generator. Cyclic voltammograms (CVs) were recorded by a PAR 273A potentiostat equipped with ohmic drop compensation system.

Before the experiments, the alloy sheet electrodes were cleaned with trichloroethylene and etched for 5 min in 5 M HCl. Deuterium was generally loaded into the alloy by potentiostatic electrolysis in the potential ranges -1.5 to -2.0 V at 25 °C (two samples nos. (2 and 9) were charged using the highest potentials) and -1.3 to -1.8 V at 90 °C, the less negative potentials being adopted for the more concentrated electrolytes. Under these conditions, the insertion currents were relatively low (less than or equal to 100 mA cm^{-2} during the first hour, to 10 to 15 mA cm^{-2} for longer electrolyses) but Li codeposition was probably minimized [14]. Deuterium extraction was performed by anodic oxidation of the deuteride at a potential in the range 0.0 to 0.4 V. Several loading–unloading runs were carried out on each alloy sample, the loading stoichiometry [D]/[Me] achieved on any run being determined later from the charge extracted and the weight of the alloy sample [12].

3. Results

3.1. Loading by D_2

The data of a typical experiment performed with an alloy sample composed of two $3.0 \times 2.0 \times 0.05$ cm^3 sheets are plotted in Fig. 1, which shows the degree of loading as [D]/[Me] ratio vs. temperature. The continuous curve represents the absorption pattern. Some absorption occurred from the highest temperatures downwards, with two peaks at approximately 500 °C and 100 °C. Correlated with this absorption, the thermocouple placed near the sample measured fluctuating temperature increases up to 20 °C above the oven temperature. As the system cooled further, most of the absorption took place between 30 and 20 °C, at which the room-temperature stable $\alpha + \beta$ phase of the deuteride formed; a temperature rise above the oven temperature was again measured by the thermocouple.

The dotted line represents the backward desorption pattern, from 20 to 900 °C. Most of the thermal decomposition occurred between approximately 40 and 70 °C. On heating the system further, deuterium was not released steadily, as the two high temperature peaks show.

The results shown in Fig. 1 were confirmed by the other loading–unloading experiments reported in Tables 1 and 2. Table 1 summarizes data on the maximum [D]/[Me] ratio achieved at 20 °C, in equilibrium with sub-atmospheric D_2. Four alloy sheet samples were used, all having the same geometrical area (about 24 cm^2) and all but one (Fig. 1) having the same thickness. In three samples, the absorption reached with either fresh or already used alloy was compared. Although the extent of absorption differed significantly from sample to sample and from run to run, the [D]/[Me] ratio averaged over the four runs performed with fresh samples ([D]/[Me] = 0.79) was very large when compared with the [D]/[Pd] ratios usually obtained from pure Pd and D_2 at 1 atm [1]. Table 2 shows the high-temperature absorption of the alloy; the two absorption peaks in Fig. 1 could be reproduced systematically.

Table 1
Deuterium content in the alloy at 20°C after reaction with D_2 at 900 mbar

Sample label	Thickness cm	Loading cycle	D to metal atom ratio	D to Pd atom ratio
a	0.05	1	0.77 ± 0.04	0.81 ± 0.04
a	0.05	2	0.76	0.80
b	0.02	1	0.89	0.94
b	0.02	2	0.64	0.67
c	0.02	1	0.63	0.66
c	0.02	2	0.42	0.44
d	0.02	1	0.88	0.93

Average weight of the samples: b–d 2.85 g; a 7.10 g.

3.2. Electrochemical insertion

Fig. 2 shows the CVs (1 mV s^{-1}) obtained in three electrolytic solutions with the same electrode, previously converted into β-deuteride ([D]/[Me] $\geq$ 0.8 as measured by exhaustive oxidation of the electrode at the end of each voltammetric run). From the slope of the current–voltage curve at the equilibrium potential on the positive sweep, it appears that the insertion–extraction of deuterium in 0.5 M LiOD is a fast (reversible) electrochemical process, which becomes slow in 0.1 M LiOD; this behavior seems to be related to alkalinity, not to the ionic strength of the solution, as the CV in 0.1 M LiOD + 0.5 M Li_2SO_4 still revealed low electrochemical reversibility.

The main characteristics of electrochemical insertion at 25 °C are illustrated in Fig. 3, which shows how the deuterium in the alloy and the coulombic efficiency varied with electrolysis time. These data were collected with two electrodes in 0.5 M LiOD and 0.1 M LiOD + 0.5 M

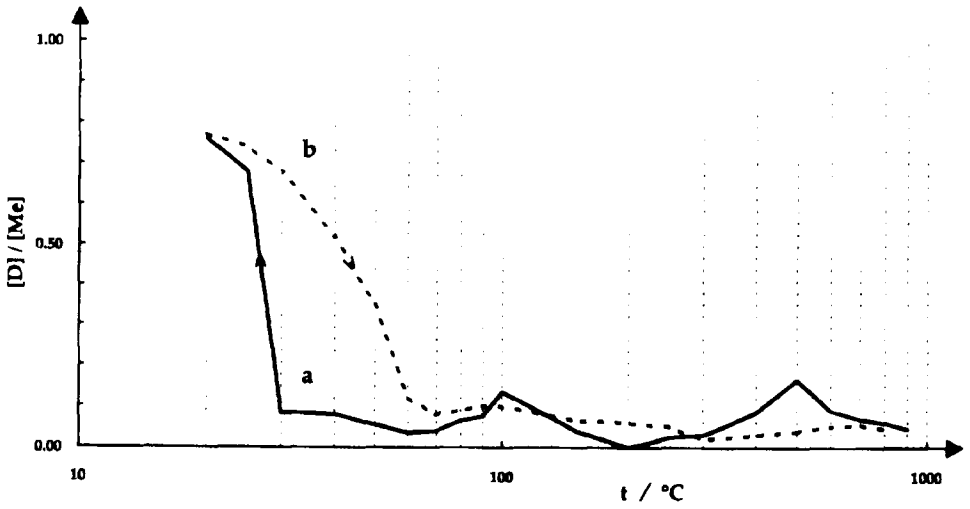

Fig. 1. D_2 absorption (———) and desorption (– – – – –) patterns for the Pd95%–Rh5% alloy.

Table 2
Deuterium content in the alloy at temperatures above room temperature as obtained from gas absorption–desorption measurements

Sample label	Mode	[D]/[Me] at 90°C	[D]/[Me] at 100°C	[D]/[Me] at 300°C	[D]/[Me] at 500°C
a	Absorption	0.08 ± 0.04	0.11 ± 0.04	0.00 ± 004	0.16 ± 0.04
a	Desorption	–	0.11	0.05	0.03
a	Absorption	0.07	0.14	0.03	0.17
b	Absorption	0.19	0.25	0.00	0.14
b	Absorption	0.18	0.25	0.08	0.21
c	Absorption	–	0.08	0.00	0.14
c	Desorption	0.14	0.10	–	–
c	Absorption	0.13	0.17	0.08	0.13
d	Absorption	0.30	0.20	0.16	0.17
Average value		0.15	0.15	0.05	0.14

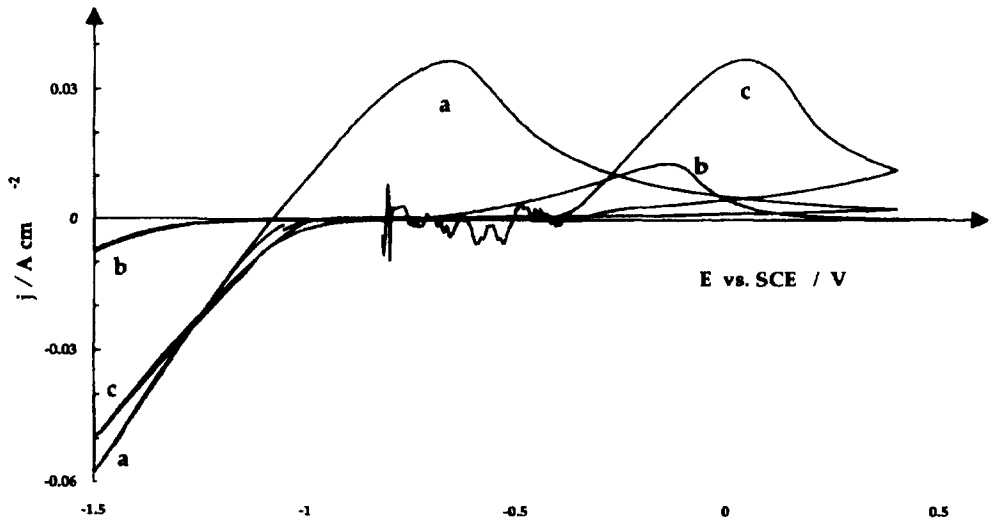

Fig. 2. CVs (1 mV s^{-1}) of a Pd95%–Rh5% deuteride electrode at 25 °C in (a) 0.5 M LiOD, (b) 0.1 M LiOD, (c) 0.1 M LiOD + 0.5 M Li_2SO_4.

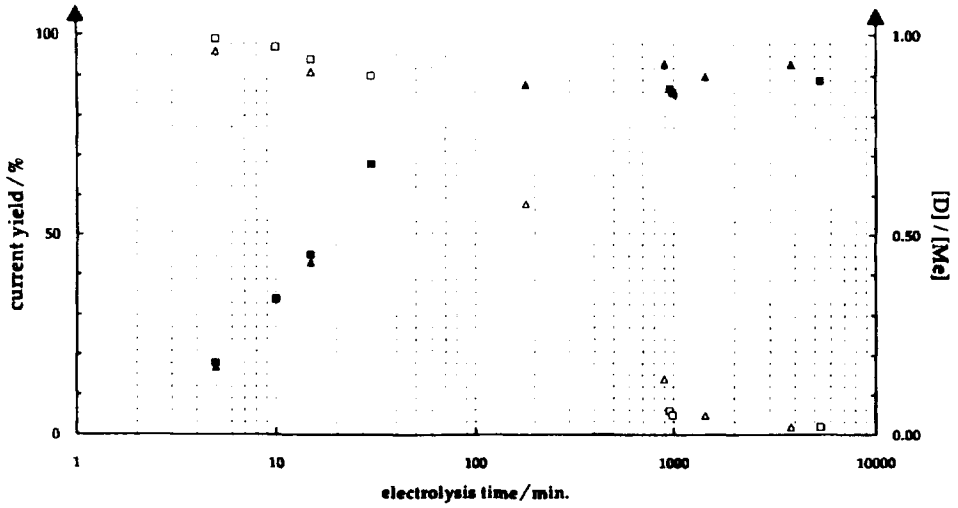

Fig. 3. Degree of loading (▲ ■, right ordinate) and current efficiency (△ □, left ordinate) vs. electrolysis time: ▲ △ 0.5 M LiOD, ■ □ 0.1 M LiOD + 0.5 M Li_2SO_4.

Table 3
Maximum deuterium loaded in the alloy at 25°C by electrolysis

Alloy sample	Electrolyte	Charging conditions		D to metal atom ratio	D to Pd atom ratio
		E/V vs. SCE	Time/min		
1 [a]	0.1 M LiOD	−2.0	5240	0.85 ± 0.01	0.89 ± 0.01
2 [a]	0.1 M LiOD	−3.5	3900	0.82	0.86
3 [a]	0.1 M LiOD	−2.5	3780	0.86	0.90
10 [a]	1.0 M LiOD	−1.6	900	0.92	0.97
11 [a]	1.0 M LiOD	−1.8	1200	0.89	0.93
13 [b]	0.1 M LiOD	−1.4	8340	0.79	0.83
14	0.1 M LiOD	−2.0	4320	0.83	0.87
15	0.1 M LiOD	−2.0	1440	0.85	0.89
16	0.1 M LiOD	−1.8	960	0.85	0.89
16	0.5 M LiOD	−1.5	3780	0.93	0.98
17	0.5 M LiOD	−1.5	1020	0.90	0.95
17	0.1 M LiOD + 0.5 M Li_2SO_4	−1.5	3720	0.86	0.90
18	0.1 M LiOD + 0.5 M Li_2SO_4	−1.5	5340	0.89	0.94

Extraction potential 0.4 V vs. SCE.
[a] Extraction potential 0.0 V vs. SCE.
[b] Thickness 0.05 cm.

Table 4
Maximum deuterium loaded in the alloy at 90°C by electrolysis

Alloy sample	Electrolyte	Charging conditions		D to metal atom ratio	D to Pd atom ratio
		E/V vs. SCE	Time/min		
13 [a]	0.1 M LiOD	−1.3	4260	0.71 ± 0.01	0.75 ± 0.01
15	0.1 M LiOD	−2.0	1080	0.75	0.79
17	0.5 M LiOD	−1.3	900	0.79	0.83
18	0.1 M LiOD + 0.5 M Li_2SO_4	−1.3	1020	0.75	0.79

Extraction potential 0.0 V vs. SCE. [a] Thickness 0.05 cm.

Li_2SO_4 respectively by a set of potentiostatic loading ($E = -1.5$ V) and unloading ($E = 0.4$ V) cycles, in which the loading time was increased at each cycle and both the corresponding [D]/[Me] ratio and the current yield percent were measured. Conversion to the β-deuteride ([D]/[Me] = 0.6 to 0.7) took place during the first hour with a current efficiency of about 90%. Deeper deuterium loading into the β-deuteride phase ([D]/[Me] $\geq$ 0.8) required

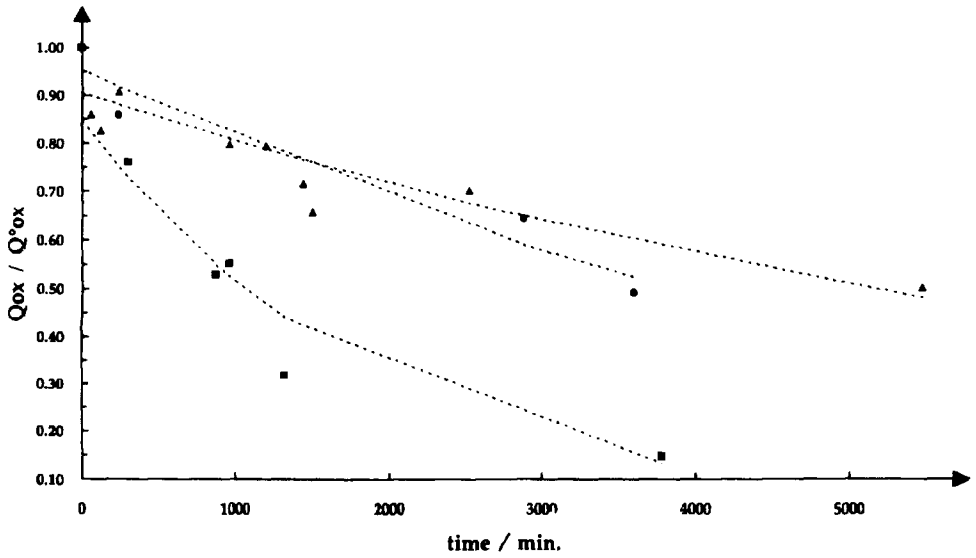

Fig. 4. Kinetics of OC decomposition of alloy deuteride electrodes at 90 °C. ▲ 0.1 M LiOD; ● 0.5 M LiOD; ■ 0.1 M LiOD + 0.5 M Li_2SO_4.

Table 5
Maximum hydrogen loaded in the alloy at 25°C by electrolysis

Alloy sample	Electrolyte	Charging conditions		H to metal atom ratio	H to Pd atom ratio
		E/V vs. SCE	Time/min		
4	0.1 M LiOH	−2.0	3960	0.90 ± 0.01	0.95 ± 0.01
5	1.0 M LiOH	−2.0	1140	0.94	0.98
6	0.1 M LiOH	−2.0	3840	0.88	0.93
7	0.1 M LiOH	−2.0	1020	0.93	0.97
8	0.1 M LiOH	−2.0	3900	0.93	0.97
9 [a]	0.1 M LiOH	−2.0	240	0.91	0.96
9	1.0 M LiOH	−1.6	330	0.95	1.00
10	1.0 M LiOH	−1.6	870	0.93	0.97

Extraction potential 0.0 V vs. SCE. [a] Extraction potential 0.4 V vs. SCE.

longer times; the maximum [D]/[Me] ratio was reached after 24 h in 0.5 M LiOD and three days later in 0.1 M LiOD + 0.5 M Li_2SO_4, the value being higher in the former than in the latter. Predictably, at high [D]/[Me] ratios, the coulombic yield of the insertion dropped, most of the discharged deuterium being converted to D_2.

The maximum [D]/[Me] ratios reached by a number of samples loaded potentiostatically in either LiOD of various concentrations or 0.1 M LiOD + 0.5 M Li_2SO_4 at 25 °C are reported in Table 3, in which the experimental conditions are also described. The maximum amount of deuterium loaded into the alloy clearly depends on the electrolytic environment, since the average [D]/[Me] ratios are approximately 0.85 in 0.1 M LiOD, approximately 0.87 in 0.1 M LiOD + 0.5 M Li_2SO_4, and greater than or equal to 0.90 in concentrated LiOD. With respect to this point, comparison of [D]/[Me] values obtained with the same alloy but in different electrolytes (samples 16 and 17) is very significant.

Table 4 shows the maximum deuterium absorbed by the alloy after electrochemical insertion at 90 °C; the [D]/[Me] ratios are 15%–20% lower than those measured at 25 °C and again show the influence of the electrolytic environment. The [D]/[Me] ratio achieved by electrolysis at 90 °C may be viewed as a loading level in equilibrium with deuterium at high activity. From examination of Fig. 1, which provides a [D]/[Me] ratio of about 0.15 in equilibrium with sub-atmospheric D_2 at 90 °C, strong thermodynamic instability can be predicted for the deuteride electrode as soon as cathodic polarization is removed. This was investigated by determining the fraction of the initial deuterium content still present in a sample when it was left at open circuit (OC) in the electrolytic solution for increasing rest times; in these experiments, electrolytic insertion did not exceed 4 to 8 h to minimize the codeposition of impurities. The data for LiOD (0.1 M or 0.5 M) and for 0.1 M LiOD + 0.5 M Li_2SO_4 are shown in Fig. 4. The OC decomposition of deuteride was faster in Li_2SO_4 than in LiOD (decomposition times for both LiOD concentrations are very close to each other); deuterium outgassing at the alloy | electrolyte interface was 1–2 orders of magnitude slower than at the alloy | gas boundary (cf. Fig. 1).

For a comprehensive view of the electrochemical insertion process, some runs were performed in light water to determine the maximum amount of hydrogen which could be loaded into the alloy at 25 °C. Conditions and results are reported in Table 5. In dilute LiOH, the [H]/[Me] ratios were slightly lower than those in concentrated LiOH, which in turn are only slightly above the [D]/[Me] values obtained in concentrated LiOD. With respect to this latter point, it is interesting to compare the data of sample 10 in D_2O (Table 3) or H_2O.

4. Discussion

Concerning the gas phase loading–unloading experiments, no strict thermodynamic meaning can be associated with the entire [D]/[Pd] vs. temperature pattern of Fig. 1. The degree of loading was in fact obtained under dynamic conditions which involved both the temperature and pressure as variables.

However, when the temperature of the system decreased below 80 °C, D_2 absorption took place under quasi-equilibrium conditions since (i) the D_2 absorbed by the sample was a fraction of all the gas contained in the reservoir and the corresponding pressure drop could not affect the absorption reaction significantly, (ii) the D_2 pressure above the sample was in large excess of the room temperature equilibrium pressure of the β-deuteride, and (iii) the average rate of spontaneous cooling was about 3 °C h^{-1}, which is slow enough compared with the diffusion time of deuterium through the sample thickness.

Therefore not only does the [D]/[Pd] ratio achieved eventually at 20 °C represent the true equilibrium value, but a near thermodynamic value can be attributed to the low temperature absorption (desorption) pattern.

In agreement with the literature data achieved under isothermal conditions [7–11] it is thus observed that deuterium storage in the alloy is significantly greater than that in pure Pd, the $\alpha + \beta$ phase of the alloy deuteride has a lower thermal stability range than the corresponding deuterides of Pd, and absorption–desorption patterns (cf. Fig. 1) show hysteresis typical of any transition in the Pd–hydrogen system.

However, it was unexpected that the [D]/[Me] ratios (Table 1) would be comparable with the values obtained by Baranowski et al. ([H]/[Me] = 0.82 to 0.91) [11] using (1) the light hydrogen isotope, and (2) very high gas pressures.

With respect to point (1), it is probably an intrinsic property of this alloy to absorb considerable amounts of either hydrogen or deuterium (see below). With respect to point (2), why under these conditions the absorption was so large, we attempt an explanation.

We believe that the metal surface is the clue to gas absorption; the alloy samples, owing to careful pre-cleaning, reached their highest surface activation. The importance of the state of the surface is stressed here by the experimental observation that "fresh" samples absorbed more deuterium than samples already used (cf. Table 1). Another factor favoring large absorption was probably the type of pathway used in our gas loading experiments, which provided interaction of the alloy with D_2 from 900 °C. Such interactions could have induced lattice disordering–ordering processes in the alloy, which affect significantly the hydrogen absorption, as recently pointed out by Flanagan and Sakamoto [13] for Pd–Mn alloys. The absorption (above the error) repeatedly measured at approximately 500 °C and 100 °C, i.e., far from the stability range of the $\alpha + \beta$ phase of the deuteride could be ascribed to similar processes. The fluctuating behavior observed here is probably associated with the parallel fluctuations of the sample temperature measured by the thermocouple, but nothing can be said about this phenomenon.

As regards the results of electrochemical insertion, it may be noted that the [D]/[Me] reached in either 0.1 M LiOD or 0.1 M LiOD + 0.5 M Li_2SO_4 does not exceed greatly the values shown in Table 1. It is again suggested that the advantage of achieving the high deuterium activity provided by the cathodic overpotential was partly offset by the state of the surface, which was far less active in the electrochemical environment than in our gas loading experiments.

A significant [D]/[Me] increase was obtained by electrochemical insertion in concentrated LiOD in which, according to the CVs of Fig. 2, the insertion–extraction process shows the highest electrochemical reversibility. This indicates that, of the three steps of HER [14],

$$e^- + M + D_2O \underset{k_{-1}}{\overset{k_1}{\rightleftharpoons}} MD_{ads} + OD^- \quad (1)$$

$$MD_{ads} + D_2O + e^- \xrightarrow{k_2} M + D_2 + OD^- \quad (2)$$

$$2MD_{ads} \xrightarrow{k_3} 2M + D_2 \quad (3)$$

step (1) is fast. This means that the main condition for correlating the thermodynamic potential of D_{ads} or D_{abs} to the applied overpotential is fulfilled better in concentrated than in dilute LiOD. In fact, according to Conway and Jerkiewicz [15], the high [D]/[Me] reached here in concentrated LiOD for appreciable-η applied is a consequence of the HER in which $k_1 \gg k_2$ and the absorption site fraction quotient $x_D/(1 - x_D)$ (within the metal) is related exponentially to the applied overvoltage. We arrive at the same conclusions when we argue according to traditional views [16,17]. The more the system is reversible the more (a fraction of) the applied overpotential correlates with an equivalent hydrogen pressure through the Nernst equation:

$$p_{D2} = \exp(-2F\eta/RT) \quad (4)$$

and therefore the high [D]/[Me] ratio reached in concentrated LiOD depends on the electrochemical insertion occurring under an equivalent deuterium pressure higher than that in dilute LiOD. The forced loading of deuterium in the alloy by electrolysis is emphasized by the large [D]/[Me] ratios at 90 °C (Table 4). It was quite surprising to observe how at OC at 90 °C, the overloaded electrodes left free D_2 much more slowly than in the alloy–gas experiments. In fact, the passage of deuterium from the metal to the exterior is not so straightforward, as it requires at least three stages: (1) diffusion of deuterium within the metal, (2) transition from absorbed to absorbed state, (3) recombination of two adsorbed atoms to a D_2 molecule. Each of these stages may become a desorption rate-determining step.

In the clean environment typical of the metal–gas experiment, a large number of surface sites were available to adsorption so that, as shown in Fig. 1, the exit of deuterium from the sample is controlled only by diffusion. Conversely, in the electrolytic environment, the number of surface sites was probably greatly reduced either by competitive adsorption of the electrolyte or by surface poisoning by codeposition of impurities during deuterium insertion, so that either stage (2) or stage (3) could have become the rate-determining step of the outgassing process. We suggest also that the double-layer structure at the alloy–deuteride boundary plays a role in accounting for the behavior shown in Fig. 4. Deuterium enters the metal lattice by adding an s electron to the collective ds band of the Pd–Rh alloy, whose free electron density rises above the original Fermi level; when dipped in an electrolyte, the alloy deuteride surface probably becomes negatively charged with respect to the solution, so that an electric field is created from the solution to the alloy. Now, if deuterium in subsurface layers is (quasi) ionic, the $D_{abs} \rightarrow D_{ads}$ transition finds an electric field barrier. Support for this view is given by recent determinations of the zero charge potential of Pd [18] which, in alkaline media, is always positive with respect to the potential of the hydride. Accordingly, the D_2 outgassing kinetics, which is faster in 0.1 M LiOD + 0.5 M Li_2SO_4 than in LiOD electrolyte (Fig. 4), may be explained by variations in the double-layer barrier induced by Li_2SO_4.

As regards the data obtained in light water, we must compare our [H]/[Me] ratio, frequently in the range 0.93–

0.95, with the maximum value of 0.91 achieved by Baranowski et al. [11] under a hydrogen pressure of 2.3×10^4 atm. This may be viewed as if under our conditions hydrogen insertion were occurring for equivalent hydrogen pressures much greater than 10^4 atm.

The effect of electrolyte concentration on maximum loading, less in H_2O than in D_2O, is obviously due to an insertion process which is always easier for the lighter than for the heavier hydrogen isotope [1]. However, the proper choice of electrolytic environment meant that it was possible to achieve similar limiting values for the [D]/[Me] and [H]/[Me] ratios, which is probably a peculiarity of this alloy with respect to pure Pd.

References

[1] F.A. Lewis, The Palladium Hydrogen System, Academic Press, London, 1967.
[2] E. Wicke and H. Brodowsky, Hydrogen in palladium and palladium alloys, in G. Alefield and J. Volke (Eds.), Topics in Applied Physics, Vol. 29, Springer, Berlin, 1978, p. 73.
[3] B.R. Coles, J. Inst. Met., 84 (1956) 346.
[4] A. Maeland and T.B. Flanagan, Can. J. Phys., 42 (1964) 2364.
[5] K. Allard, A. Maeland, J.W. Simons and T.B. Flanagan, J. Phys. Chem., 72 (1968) 136.
[6] H. Brodowsky, Ber. Bunsenges. Phys. Chem., 76 (1972) 740.
[7] H. Brodowsky and H. Husemann Ber. Bunsenges. Phys. Chem., 70 (1966) 626.
[8] J. Barton, J.A.S. Green, and F.A. Lewis, Trans. Faraday Soc., 62 (1966) 960.
[9] J.A.S. Green and F.A. Lewis, Trans. Faraday Soc., 62 (1966) 971.
[10] T.B. Flanagan, B. Baranowski and S. Majchrza, J. Phys. Chem., 74 (1970) 4299.
[11] B. Baranowski, S. Majchrza and T.B. Flanagan, J. Phys. Chem. 77 (1973) 35.
[12] G. Mengoli, M. Fabrizio, C. Manduchi and G. Zannoni, J. Electroanal. Chem., 350 (1993) 57.
[13] T.-B. Flanagan and Y. Sakamoto, Platinum Met. Rev., 37 (1993) 26.
[14] M. Enyo and P.C. Bizwas, J. Electroanal. Chem., 335 (1992) 309.
[15] B.E. Conway and G. Jerkiewicz, J. Electroanal. Chem., 357 (1993) 47.
[16] M. Enyo, HER on electrocatalytically active metals, in B.E. Conway, J.O'M. Bockris, E. Yeager, S.U.M. Khan and R. White (Eds.), Comprehensive Treatise of Electrochemistry, Vol. 7, Plenum, New York, 1983, p. 241.
[17] M. Enyo and P.C. Biswas, J. Electroanal. Chem., 357 (1993) 67.
[18] M. Seo and M. Aomi, J. Electrochem. Soc., 139 (1992) 1087.